Zeolite Nanocages

Deutsche Ausgabe: DOI: 10.1002/ange.201505508
Internationale Ausgabe: DOI: 10.1002/anie.201505508

Confinement of Ionic Liquids in Nanocages: Tailoring the Molecular Sieving Properties of ZIF-8 for Membrane-Based CO_2 Capture

Yujie Ban, Zhengjie Li, Yanshuo Li, Yuan Peng, Hua Jin, Wenmei Jiao, Ang Guo, Po Wang, Qingyuan Yang,* Chongli Zhong, and Weishen Yang**

Abstract: *Fine-tuning of effective pore size of microporous materials is necessary to achieve precise molecular sieving properties. Herein, we demonstrate that room temperature ionic liquids can be used as cavity occupants for modification of the microenvironment of MOF nanocages. Targeting CO_2 capture applications, we tailored the effective cage size of ZIF-8 to be between CO_2 and N_2 by confining an imidazolium-based ionic liquid [bmim][Tf_2N] into ZIF-8's SOD cages by in-situ ionothermal synthesis. Mixed matrix membranes derived from ionic liquid-modified ZIF-8 exhibited remarkable combinations of permeability and selectivity that transcend the upper bound of polymer membranes for CO_2/N_2 and CO_2/CH_4 separation. We observed an unusual response of the membranes to varying pressure, that is, an increase in the CO_2/CH_4 separation factor with pressure, which is highly desirable for practical applications in natural gas upgrading.*

Capturing carbon dioxide is of great importance to make cuts in greenhouse gas emissions. Membrane-based CO_2 capture is superior to the current chemical absorption techniques in terms of energy consumption. Polymeric membranes, in particular, have proven successful in natural gas sweetening (NGS) and enhanced oil recovery (EOR).[1] In general, however, polymeric gas separation membranes are subject to a trade-off between permeability and selectivity, known as Robeson's upper bound.[2] Membranes derived from molecular sieve materials are expected to overcome this limitation based on size exclusion mechanisms. In this regard, fine-tuning of their pore size is necessary to achieve precise molecular sieving properties. A classic example is the stepwise increase of the pore size of A-type zeolite from 3 Å to 5 Å by ion-exchange.[3] Microporous metal–organic frameworks (MOFs) are a growing class of molecular sieves, and promote the generation of separating membranes.[4] Compared with zeolites, a distinct advantage of MOFs is their designable synthesis and diverse post-modification options, which provide a number of possibilities for altering their effective pore sizes. Post-synthesis modification,[5] metal substitution,[6] and ligand exchange[7] have been reported to be effective in altering the aperture size of several types of MOFs. The breaking and forming of bonds in the post-modifications, however, might lead to transformation of the crystal structures and dissolution of parent materials.[6]

Herein, we present a way for tailoring the molecular sieving properties of cage-type MOFs, namely through modification of the microenvironment of the MOF nanocages by introduction of cavity occupants (Scheme 1). Room-temperature ionic liquids (RTILs) were used as the cavity occupants, considering their negligible vapor pressure, high thermal stability, good affinity to CO_2,[8a] and potential use as solvents for ionothermal synthesis.[8b] The ionic liquid 1-butyl-3-methylimidazolium bis(trifluoromethyl-sulfonyl) imide ([bmim][Tf_2N]), was chosen given that [Tf_2N](−) is favorable for CO_2 adsorption[8a] and [bmim](+) is bulky enough for an efficient cavity occupancy. Zeolitic imidazolate framework-8 (ZIF-8), a cage-type microporous MOF with high stability, was chosen as the host material.[9] ZIF-8 is formed by bridging 2-methylimidazolate (mim) anions and zinc cations with sodalite (SOD) topology. The large SOD cages (1.12 nm) are

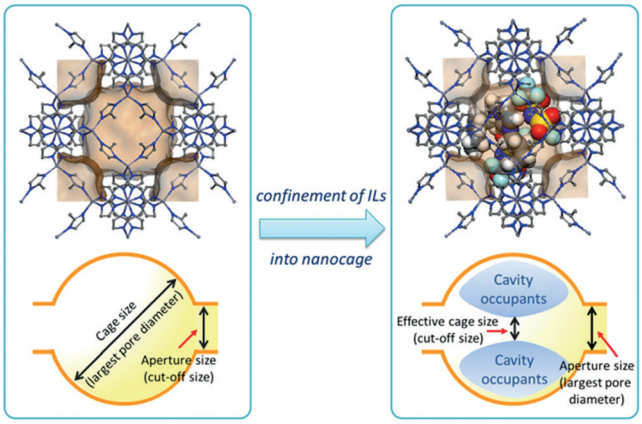

Scheme 1. Illustration of the cavity-occupying concept for tailoring the molecular sieving properties of ZIF-8 by incorporation of RTILs. The cut-off size shifts from the aperture size of six-membered ring to the reduced effective cage size by confinement of [bmim][Tf_2N] in a ZIF-8's SOD cage.

[*] Y. Ban, Prof. Dr. Y. Li, Y. Peng, H. Jin, W. Jiao, A. Guo, P. Wang, Prof. Dr. W. Yang
State Key Laboratory of Catalysis
Dalian Institute of Chemical Physics, CAS
457 Zhongshan Road, Dalian 116023 (China)
E-mail: leeys@dicp.ac.cn
yangws@dicp.ac.cn
Z. Li, Prof. Dr. Q. Yang, Prof. Dr. C. Zhong
State Key Laboratory of Organic–Inorganic Composites
Beijing University of Chemical Technology
15 Beisanhuan East Road, Beijing 100029 (China)
E-mail: qyyang@mail.buct.edu.cn
Y. Ban, Y. Peng, H. Jin, W. Jiao, A. Guo, P. Wang
University of Chinese Academy of Sciences
19A Yuquan Road, Beijing 100049 (China)

Supporting information for this article is available on the WWW under http://dx.doi.org/10.1002/anie.201505508.

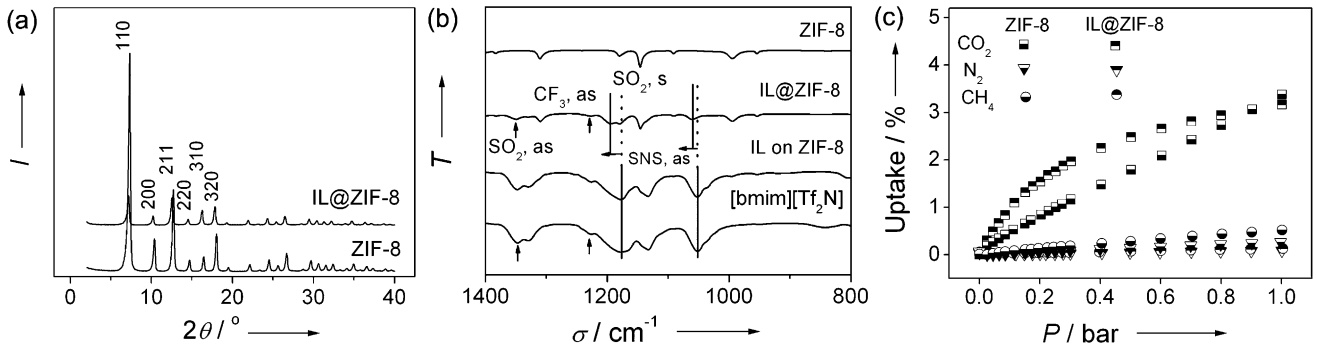

Figure 1. PXRD patterns (a) and ATR-FTIR spectra (b) of ZIF-8 and IL@ZIF-8. c) Adsorption isotherms of CO_2, N_2 and CH_4 on ZIF-8 and IL@ZIF-8 at 298 K.

connected through small apertures (0.34 nm). The latter are expected to enable molecular sieving of CO_2 (0.33 nm) over more bulky molecules, such as N_2 (0.364 nm) and CH_4 (0.38 nm). However, as a result of flexible pore architecture (swing effect in the imidazolate linkers),[10] ZIF-8 membranes exhibit only moderate CO_2 selectivities.[11] Therefore, a further reduction of the cut-off size of ZIF-8 is needed.

We carried out an ionothermal synthesis for in-situ incorporation of RTILs into the nanocages of ZIF-8, that is, the RTILs act as both solvent and cavity occupants. For the synthesis, zinc nitrate and mim were dissolved into [bmim]-[Tf_2N]. The solution was stirred at room temperature for 24 hrs. The product was recovered by centrifugation. Complete washing with methanol is necessary to remove [bmim]-[Tf_2N] coated on the outer-surface of the products. (Supporting Information, Figure S1).

As shown in the powder X-ray diffraction (XRD) patterns (Figure 1 a), the crystalline lattice structure of the product coincides with that of ZIF-8. The decrease in the relative intensity of low Miller-index planes (110) suggests that the electron density inside the nanocages of ZIF-8 changed as a result of incorporation of [bmim][Tf_2N], which is in agreement with the modelling results (Supporting Information, Figure S2). The product hereafter is denoted as IL@ZIF-8.

The attenuation total reflectance-Fourier transform infrared (ATR-FTIR) spectra (Figure 1 b) provide further evidence that successful confinement of ILs into ZIF-8 was achieved. Four vibration bands at 1350, 1230, 1200, and 1065 cm^{-1}, respectively, appear in the IL@ZIF-8, corresponding to the vibrations of [Tf_2N](−) anion: SO_2 asymmetric stretching (as), CF_3 asymmetric stretching (as), SO_2 symmetric stretching (s), and SNS asymmetric stretching (as) modes, respectively.[12] Compared with bulk IL and IL coated on the outer-surface of ZIF-8, blue shifts of the SO_2 symmetric stretching band (from 1175 to 1200 cm^{-1}) and SNS asymmetric stretching band (from 1050 to 1065 cm^{-1}) were observed, which can be explained by the strong interaction of N and S atoms of [Tf_2N](−) with the metal nodes of ZIF-8, and further supported by molecular dynamic (MD) simulations (Supporting Information, Figures S3, S4 and Tables S1–S3).

The molar ratio of IL to ZIF-8 was 0.235, determined by ^1H NMR characterization (Supporting Information, Figure S5). This can be translated into a confinement ratio of 1.4 ILs per SOD cage, coinciding with the TG results (Supporting Information, Figure S6 and Table S4).

IL@ZIF-8 displays a type-I isotherm for adsorption of N_2 at 77 K (Supporting Information, Figure S7). Owing to the space-occupying effect of ILs in the nanocages of ZIF-8, the N_2 adsorption amount declined evidently, and accordingly, the Brunauer–Emmett–Teller (BET) surface areas decreased from 1379 $m^2 g^{-1}$ for ZIF-8 to 374 $m^2 g^{-1}$ for IL@ZIF-8 (Table 1). Theoretical calculations provide further insight into the pore structural evolution of ZIF-8 at a confinement ratio of 1.4 ILs per SOD cage. The largest pore diameter (LPD) in the pristine ZIF-8 was found to be 1.12 nm, corresponding to the diameter of SOD cage (Scheme 1). In contrast, the position of the LPD of IL@ZIF-8 moved to the region near the six-membered ring, and the value decreased to 0.59 nm (Table 1), which is also the effective cut-off size of the pristine ZIF-8. The pore size distribution also indicated that the effective cage size of ZIF-8 was remarkably reduced after incorporation of ILs (Supporting Information, Figure S8).

Table 1: Experimental and modelling results of gas adsorption on ZIF-8 and IL@ZIF-8.

Sample	BET	Pore volume[a]	LPD[c]	Ideal adsorption selectivity[d]	
	[$m^2 g^{-1}$]	[$mL g^{-1}$]	[nm]	CO_2/N_2	CO_2/CH_4
ZIF-8	1379 (1462)[b]	0.67 (0.55)[b]	1.12	19	7.5
IL@ZIF-8	374 (263)[b]	0.18 (0.14)[b]	0.59	100	41

[a] Analyzed with the Horváth–Kawazoe (HK) method; [b] Theoretical calculation results are given in the parentheses; [c] Largest pore diameter (LPD) obtained theoretically; [d] Calculated using the initial slope in the Henry region of isotherms at 298 K based on Henry's law.

The adsorption isotherms of CO_2, N_2, and CH_4 on ZIF-8 and IL@ZIF-8 were measured using an Intelligent Gravimetric Analyzer (IGA) at 298 K (Figure 1 c). The sorption amount of N_2 and CH_4 of IL@ZIF-8 was decreased as a result of the reduced pore volume. In contrast, the uptake of CO_2 was enhanced, especially in the relative low pressure region, which can be attributed to the good solubility of CO_2 in [bmim][Tf_2N]. The ideal adsorption selectivity of IL@ZIF-

8 was calculated from the ratio of the initial slopes in the Henry region of the isotherms (Supporting Information, Figure S9). A significant improvement in CO_2/N_2 and CO_2/CH_4 adsorption selectivities was achieved (Table 1). In particular, the CO_2/N_2 selectivity of IL@ZIF-8 is up to 100, among the best of CO_2-philic adsorbents (Supporting Information, Table S5) and far exceeding that of ZIF-8 (19; see Table 1) and bulk ILs (32; see the Supporting Information, Table S6). A synergistic effect between confined ILs and ZIF-8's nanocages might account for this remarkable enhancement.

Mixed matrix membranes (MMMs) with MOFs or zeolite nanoparticles as fillers have great potential for energy-efficient gas separation.[13] In light of the above results, we used IL@ZIF-8 nanoparticles as fillers for fabricating MMMs. Here, polysulfone (PSF) was used as polymer matrix in consideration of its low price, good processability, and high plasticization pressure.[14] Apart from the MMMs containing ZIF-8 nanoparticles that were physically mixed with ILs, no diffraction peaks in XRD patterns were observed for the IL@ZIF-8 MMMs (Supporting Information, Figure S10). This can be seen as evidence that ILs were still confined in the nanocages of ZIF-8 after membrane preparation, considering that the ILs inside the nanocages leads to a decrease in the peak intensity of ZIF-8 (Figure 1a).

The membranes were sealed into Wicke–Kallenbach cells to measure the permeability and selectivity of CO_2, N_2, and CH_4 for both binary mixed gases and single gases. Based on the analysis of different filler loadings, we found a volume fraction of 6% IL@ZIF-8 optimized the CO_2 separation performances of the MMMs. Statistical analysis, including ANOVA and t-test, suggested a significant effect of volume fraction of fillers on membrane selectivity (Supporting Information, Tables S7 and S8).

Figure 2a shows the single gas permeability through an IL@ZIF-8 MMM and a pure PSF membrane. For IL@ZIF-8 MMMs, the permeability of H_2, CO_2, and O_2 increased by 61, 48, and 39%, respectively, but that of N_2 or CH_4 hardly changed. As a result, the ideal selectivities (the ratio of single gas permeability) of H_2/N_2, H_2/CH_4, O_2/N_2, CO_2/N_2, and CO_2/CH_4 were remarkably improved (Supporting Information, Table S9). We also conducted a controlled experiment using ZIF-8 as fillers, and found enhanced permeabilities but constant or decreased selectivities for all the gases (Supporting Information, Table S9). This result reflects the reduced effective pore opening of ZIF-8 after incorporation of ILs.

The IL@ZIF-8 MMMs (volume fraction 6%) were also tested for the separation of CO_2 from CO_2/CH_4 as well as CO_2/N_2 mixtures. Controlled experiments were also conducted including pure PSF membranes, ZIF-8 MMMs, IL MMMs (ILs as fillers), and IL-ZIF-8 MMMs (ZIF-8 was physically mixed with ILs and used as fillers). As shown in Figure 2b and c, the addition of highly porous ZIF-8 nanoparticles into PSF resulted in a remarkable increase in permeabilities for all types of gases, but constant or slightly decreased CO_2 selectivities. Similar phenomena have been seen in other MOF-based MMMs.[13c] The addition of IL@ZIF-8 led to a greater than 50% increase in permeability for CO_2 and, at the same time, cut down the permeabilities of CH_4 and N_2. Furthermore, the permeability of H_4 and N_2 in the mixtures was much lower than in the single-component, while there is little difference for the CO_2 permeability, providing that separation factor (calculated as the permeate-to-retentate composition ratio of fast gas, divided by the same ratio of slow gas) was much higher than the corresponding ideal selectivity (Figure 2a; Supporting Information, Table S9). An explanation for this phenomenon is that in the pores of IL@ZIF-8, CH_4 and N_2 have lower adsorption and mobility compared with CO_2, resulting in a crowding-out effect. This phenomenon has been extensively investigated in the field of zeolite membranes.[15] Compared with pure PSF membranes, an increase in gas permeability but decrease in CO_2 selectivity was observed in IL MMMs. This might be attributed to the higher permeability of CO_2 and CH_4 through the bulk ILs, consistent with other reports.[16] The experimental results obtained from these controlled experiment with IL-ZIF-8 MMMs provide indirect evidence that the ILs were still confined in the nanocages of ZIF-8 during the preparation of IL@ZIF-8 MMMs. Statistical analysis suggested a highly significant effect of filler type on membrane selectivity (Supporting Information, Tables S10 and S11).

High-pressure CO_2 is known to swell and plasticize polymers, leading to a permanent loss of selectivity of polymer membranes.[17] To evaluate their stability against plasticization, the membranes were tested for the separation of CO_2/CH_4 and CO_2/N_2 gas mixtures (50/50 vol.%) at elevated pressures (up to 20 bar). For pure PSF membrane, we observed a continuous decrease in CO_2/CH_4 separation

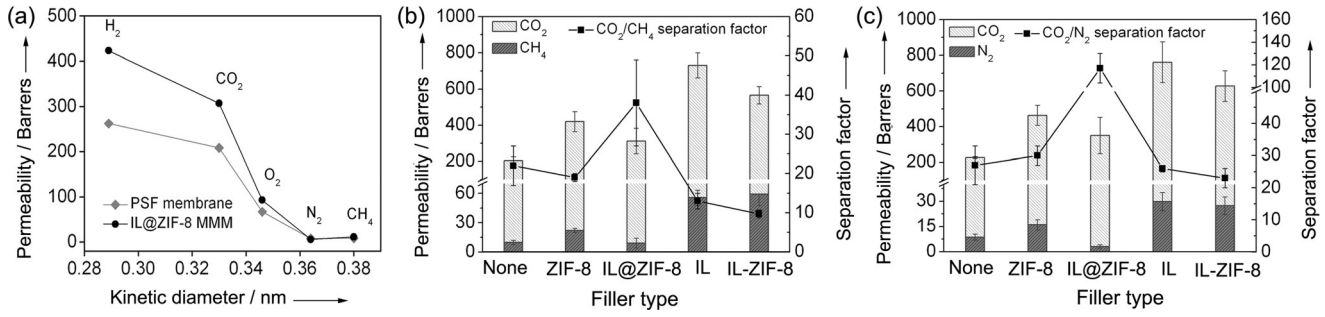

Figure 2. a) Single gas permeation through a PSF membrane and an IL@ZIF-8 MMM (volume fraction 6%). Mixed gas separation performances toward equimolar CO_2/CH_4 (b) and CO_2/N_2 (c) of PSF membrane, ZIF-8 MMMs, IL@ZIF-8 MMMs, IL MMMs (ILs as fillers), and IL-ZIF-8 MMMs (ZIF-8 was physically mixed with ILs and used as fillers). Feed pressure of 6 bar, 303 K. 1 Barrer $= 10^{-10}$ cm^3 cm cm^{-2} s^{-1} cm Hg^{-1}.

factor with increasing pressure (see Figure S11 in the Supporting Information). The IL@ZIF-8 MMMs, on the contrary, showed an unusual behaviour that CO_2 selectivity increases with pressure (Figure S11). The CO_2/CH_4 separation factor increased to 66 at feed pressure of 20 bar, wherein the fugacity of CO_2 in the feed (9.2 bar) lies already in the range of interest for industrial applications (Supporting Information, Table S12). As for the CO_2/N_2 gas pair, pure PSF membrane again showed decreased CO_2 selectivity with increasing pressure (Supporting Information, Figure S12). For the IL@ZIF-8 MMMs, the CO_2/N_2 separation factor reached a maximum value of 152 at 10 bar (Supporting Information, Figure S12). The unusual response of IL@ZIF-8 MMMs to varying pressure is highly desirable for practical applications with compressed feed streams. Recently, Gascon et al. observed similar phenomenon in MMMs composed of NH_2-MIL-53(Al) nanocrystals[18a] and Cu-BDC nanosheets.[18b] They attributed the increased CO_2 selectivity at high pressures to the intrinsic separation properties of the fillers. We also hypothesize that the molecular sieving capacity of IL@ZIF-8 might account for this anomalous phenomenon.

Figure 3 compares the IL@ZIF-8 MMMs with the 2008 Robeson's upper bound of polymeric membranes for CO_2/CH_4 and CO_2/N_2 gas pairs, respectively. Some representative membranes from the literature are also included. For both the gas pairs, the IL@ZIF-8 MMMs show remarkable combinations of permeability and selectivity that transcend the upper bound of polymer membranes. They show superior performances compared with the supported ionic liquid ([bmim]-[Tf_2N]) membrane (SILM)[19a] and the poly (ionic liquid) membrane that contains ZIF-8 nanoparticles.[19b] Furthermore, the IL@ZIF-8 MMMs exhibited excellent stability in a long term test (Supporting Information, Figure S13). It should be noted that implementation of the permeation data using the Maxwell equation indicates that an interfacial void might exist in the MMMs (Supporting Information, Table S13). Therefore, an optimization of the interfacial morphology and interaction between the polymer phase and filler phase would lead to a further enhancement in membrane performance.

In summary, we confined RTIL [bmim][Tf_2N] into the nanocages of ZIF-8 through an in-situ ionothermal synthesis method, achieving an effective alteration of the molecular sieving properties of ZIF-8 for CO_2 separation. Mixed matrix membranes containing IL-modified ZIF-8 showed great potential in membrane-based CO_2 captures such as natural gas sweetening, biogas upgrading, and post-combustion CO_2 capture. We believe that the cavity occupying concept can be extended to other types of MOFs and ionic liquids. It is also possible to achieve a target-oriented alteration of MOF's cut-off size through choosing ILs with proper chain length or controlling the confinement ratios.

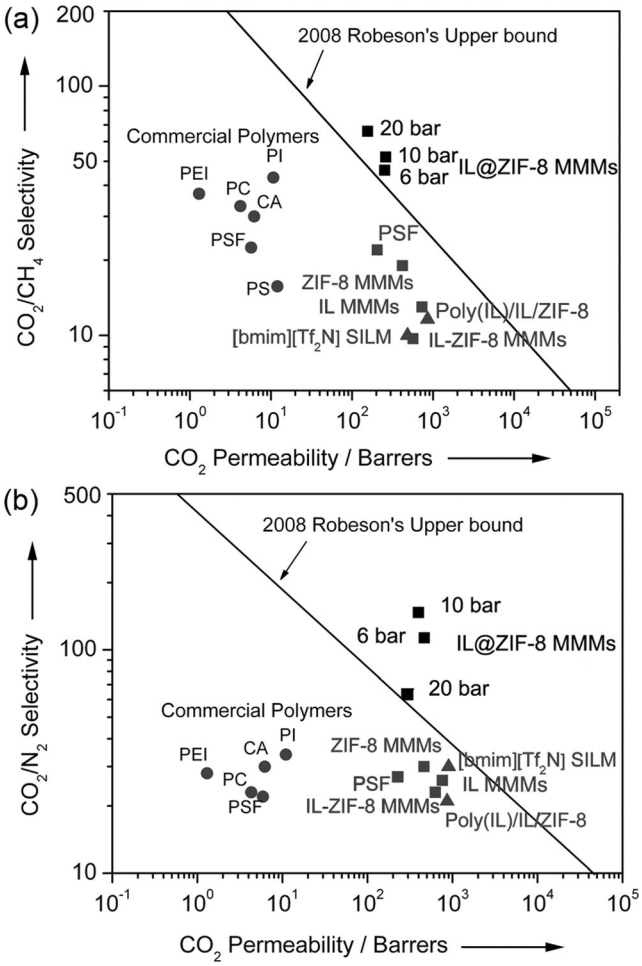

Figure 3. The plots of selectivity versus permeability for CO_2/CH_4 (a) and CO_2/N_2 (b) gas pairs, respectively. Filled circles: data for commercial polymers, see Ref. [19c]. Filled squares: results from this work. Filled triangles: results from other works, see Ref. [19a] for [bmim]-[Tf_2N] SILM and Ref. [19b] for poly (IL)/IL/ZIF-8 membranes, respectively.

Experimental Section

An ionothermal synthesis was carried out for in-situ incorporation of RTILs into the nanocages of ZIF-8. The reactant $Zn(NO_3)_2{\cdot}6H_2O$ (1.798 g) and mim (4.000 g) were dissolved in approximately 60 mL of [bmim][Tf_2N] with the assistance of ultrasonic bath, and successively stirred at room temperature for 24 hrs. Then the sample was separated using centrifugation and washed with methanol.

The mixed matrix membranes (MMMs) were obtained by the dip-coating method using asymmetric gamma-alumina discs (Inocermic GmbH, Germany) as supports. The membrane solution was prepared by mixing IL@ZIF-8 with a polysulfone (PSF)-chloroform solution under vigorous stirring. More experimental details, MD simulations and characterizations of materials and membranes are provided in the Supporting Information.

Acknowledgements

This work was supported by the National Science Fund (21176231, 21006101, 21276249, 21136001, and 21322603) and the Key Research Programme of the Chinese Academy of Science (Grant No. KGZD-EW-T05).

Keywords: CO_2 capture · confinement · ionic liquids · molecular sieving · ZIF-8

How to cite: *Angew. Chem. Int. Ed.* **2015**, *54*, 15483 – 15487
Angew. Chem. **2015**, *127*, 15703 – 15707

[1] Y. Zhang, J. Sunarso, S. Liu, R. Wang, *Int. J. Greenhouse Gas Control* **2013**, *12*, 84 – 107.
[2] L. M. Robeson, *J. Membr. Sci.* **2008**, *320*, 390 – 400.
[3] D. W. Breck, W. G. Eversole, R. M. Milton, T. B. Reed, T. L. Thomas, *J. Am. Chem. Soc.* **1956**, *78*, 5963 – 5971.
[4] a) M. Eddaoudi, J. Kim, N. Rosi, D. Vodak, J. Wachter, M. O'Keeffe, O. M. Yaghi, *Science* **2002**, *295*, 469 – 472; b) K. Sumida, D. L. Rogow, J. A. Mason, T. M. McDonald, E. D. Bloch, Z. R. Herm, T.-H. Bae, J. R. Long, *Chem. Rev.* **2012**, *112*, 724 – 781; c) Y. Peng, Y. Li, Y. Ban, H. Jin, W. Jiao, X. Liu, W. Yang, *Science* **2014**, *346*, 1356 – 1359; d) B. Seoane, J. Coronas, I. Gascon, M. E. Benavides, O. Karvan, J. Caro, F. Kapteijn, J. Gascon, *Chem. Soc. Rev.* **2015**, *44*, 2421 – 2454.
[5] Y.-S. Bae, O. K. Faha, J. T. Hupp, R. Q. Snurr, *J. Mater. Chem.* **2009**, *19*, 2131 – 2134.
[6] Y. Ban, Y. Li, Y. Peng, H. Jin, W. Jiao, X. Liu, W. Yang, *Chem. Eur. J.* **2014**, *20*, 11402 – 11409.
[7] a) O. Karagiaridi, M. B. Lalonde, W. Bury, A. A. Sarjeant, O. K. Farha, J. T. Hupp, *J. Am. Chem. Soc.* **2012**, *134*, 18790 – 18796; b) J. A. Thompson, N. A. Brunelli, R. P. Lively, J. R. Johnson, C. W. Jones, S. Nair, *J. Phys. Chem. C* **2013**, *117*, 8198 – 8207; c) J. A. Thompson, J. T. Vaughn, N. A. Brunelli, W. J. Koros, C. W. Jones, S. Nair, *Microporous Mesoporous Mater.* **2014**, *192*, 43 – 51.
[8] a) M. Hasib-ur-Rahmana, M. Siaj, F. Larachi, *Chem. Eng. Process.* **2010**, *49*, 313 – 322; b) R. E. Morris, *Chem. Commun.* **2009**, 2990 – 2998.
[9] a) K. S. Park, Z. Ni, A. P. Côté, J. Y. Choi, R. Huang, F. J. Uribe-Romo, H. K. Chae, M. O'Keeffe, O. M. Yaghi, *Proc. Natl. Acad. Sci. USA* **2006**, *103*, 10186 – 10191; b) K. Fujie, T. Yamada, R. Ikeda, H. Kitagawa, *Angew. Chem. Int. Ed.* **2014**, *53*, 11302 – 11305; *Angew. Chem.* **2014**, *126*, 11484 – 11487.
[10] D. Fairen-Jimenez, S. A. Moggach, M. T. Wharmby, P. A. Wright, S. Parsons, T. Düren, *J. Am. Chem. Soc.* **2011**, *133*, 8900 – 8902.
[11] H. Bux, F. Liang, Y. Li, J. Cravillon, M. Wiebcke, J. Caro, *J. Am. Chem. Soc.* **2009**, *131*, 16000 – 16001.
[12] M. Sobota, I. Nikiforidis, W. Hieringer, N. Paape, M. Happel, H.-P. Steinrück, A. Görling, P. Wasserscheid, M. Laurin, J. Libuda, *Langmuir* **2010**, *26*, 7199 – 7207.
[13] a) B. Zornoza, O. Esekhile, W. J. Koros, C. Téllez, J. Coronas, *Sep. Purif. Technol.* **2011**, *77*, 137 – 145; b) A. L. Khan, C. Klaysom, A. Gahlaut, I. F. J. Vankelecom, *J. Membr. Sci.* **2013**, *447*, 73 – 79; c) Y. Dai, J. R. Johnson, O. Karvan, D. S. Sholl, W. J. Koros, *J. Membr. Sci.* **2012**, *401 – 402*, 76 – 82.
[14] H. Julian, I. G. Wenten, *J. Eng.* **2012**, *2*, 484 – 495.
[15] C. J. Gump, R. D. Noble, J. L. Falconer, *Ind. Eng. Chem. Res.* **1999**, *38*, 2775 – 2781.
[16] L. Liang, Q. Gan, P. Nancarrow, *J. Membr. Sci.* **2014**, *450*, 407 – 417.
[17] J. D. Wind, S. M. Sirard, D. R. Paul, P. F. Green, K. P. Johnston, W. J. Koros, *Macromolecules* **2003**, *36*, 6433 – 6441.
[18] a) B. Zornoza, A. Martinez-Joaristi, P. Serra-Crespo, C. Tellez, J. Coronas, J. Gascon, F. Kapteijn, *Chem. Commun.* **2011**, *47*, 9522 – 9524; b) T. Rodenas, I. Luz, G. Prieto, B. Seoane, H. Miro, A. Corma, F. Kapteijn, F. X. Llabrés i Xamena, J. Gascon, *Nat. Mater.* **2015**, *14*, 48 – 55.
[19] a) L. A. Neves, J. G. Crespo, I. M. Coelhoso, *J. Membr. Sci.* **2010**, *357*, 160 – 170; b) L. Hao, P. Li, T. Yang, T.-S. Chung, *J. Membr. Sci.* **2013**, *436*, 221 – 231; c) V. Abetz, T. Brinkmann, M. Dijkstra, K. Ebert, D. Fritsch, K. Ohlrogge, D. Paul, K.-V. Peinemann, S. Pereira-Nunes, N. Scharnagl, M. Schossig, *Adv. Eng. Mater.* **2006**, *8*, 328 – 358.

Received: June 15, 2015
Revised: October 6, 2015
Published online: October 30, 2015

